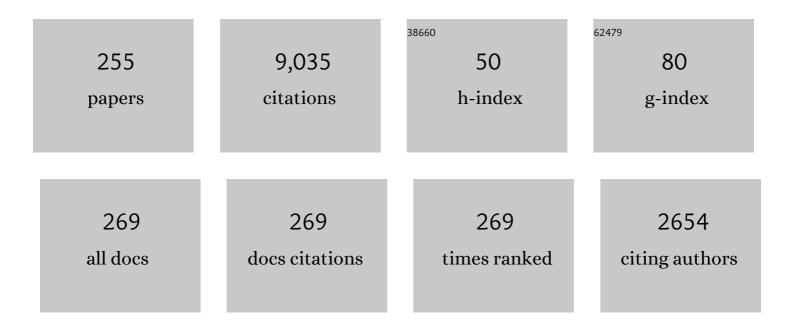


List of Publications by Year in descending order

Source: https://exaly.com/author-pdf/3098605/publications.pdf

Version: 2024-02-01



LVIIII

#	Article	IF	CITATIONS
1	Pre-earthquake ionospheric anomalies registered by continuous GPS TEC measurements. Annales Geophysicae, 2004, 22, 1585-1593.	0.6	408
2	Variations of ionospheric total electron content during the Chi-Chi Earthquake. Geophysical Research Letters, 2001, 28, 1383-1386.	1.5	272
3	Seismo-ionospheric signatures prior to M≥6.0 Taiwan earthquakes. Geophysical Research Letters, 2000, 27, 3113-3116.	1.5	250
4	A statistical investigation of preearthquake ionospheric anomaly. Journal of Geophysical Research, 2006, 111, .	3.3	242
5	Seismoionospheric GPS total electron content anomalies observed before the 12 May 2008 <i>M</i> _{<i>w</i>} 7.9 Wenchuan earthquake. Journal of Geophysical Research, 2009, 114, .	3.3	235
6	Theoretical study of the low- and midlatitude ionospheric electron density enhancement during the October 2003 superstorm: Relative importance of the neutral wind and the electric field. Journal of Geophysical Research, 2005, 110, .	3.3	185
7	lonospheric disturbances triggered by the 11 March 2011 <i>M</i> 9.0 Tohoku earthquake. Journal of Geophysical Research, 2011, 116, n/a-n/a.	3.3	173
8	Motions of the equatorial ionization anomaly crests imaged by FORMOSATâ€3/COSMIC. Geophysical Research Letters, 2007, 34, .	1.5	161
9	Plausible effect of atmospheric tides on the equatorial ionosphere observed by the FORMOSAT-3/COSMIC: Three-dimensional electron density structures. Geophysical Research Letters, 2007, 34, .	1.5	158
10	Longitudinal structure of the equatorial ionosphere: Time evolution of the fourâ€peaked EIA structure. Journal of Geophysical Research, 2007, 112, .	3.3	134
11	Giant ionospheric disturbances excited by the M9.3 Sumatra earthquake of 26 December 2004. Geophysical Research Letters, 2006, 33, .	1.5	128
12	A statistical analysis of ionospheric anomalies before 736 <i>M</i> 6.0+ earthquakes during 2002-2010. Journal of Geophysical Research, 2011, 116, n/a-n/a.	3.3	123
13	lonospheric total electron content response to solar eclipses. Journal of Geophysical Research, 1999, 104, 12657-12668.	3.3	101
14	lonospheric GPS total electron content (TEC) disturbances triggered by the 26 December 2004 Indian Ocean tsunami. Journal of Geophysical Research, 2006, 111, .	3.3	101
15	Midlatitude summer nighttime anomaly of the ionospheric electron density observed by FORMOSATâ€3/COSMIC. Journal of Geophysical Research, 2010, 115, .	3.3	101
16	Statistical analysis of ULF seismomagnetic phenomena at Kakioka, Japan, during 2001–2010. Journal of Geophysical Research: Space Physics, 2014, 119, 4998-5011.	0.8	97
17	Total Electron Content Obtained by Using the Global Positioning System. Terrestrial, Atmospheric and Oceanic Sciences, 1996, 7, 107.	0.3	96
18	Occurrence probability and amplitude of equatorial ionospheric irregularities associated with plasma bubbles during low and moderate solar activities (2008–2012). Journal of Geophysical Research: Space Physics, 2014, 119, 1186-1199.	0.8	89

#	Article	IF	CITATIONS
19	Seasonal variations of the ionospheric total electron content in Asian equatorial anomaly regions. Journal of Geophysical Research, 2001, 106, 30363-30369.	3.3	86
20	Threeâ€dimensional ionospheric electron density structure of the Weddell Sea Anomaly. Journal of Geophysical Research, 2009, 114, .	3.3	86
21	Global 3â€Ð ionospheric electron density reanalysis based on multisource data assimilation. Journal of Geophysical Research, 2012, 117, .	3.3	85
22	Rapid Conjugate Appearance of the Giant Ionospheric Lamb Wave Signatures in the Northern Hemisphere After Hungaâ€Tonga Volcano Eruptions. Geophysical Research Letters, 2022, 49, .	1.5	83
23	Space Weather Observations by GNSS Radio Occultation: From FORMOSATâ€3/COSMIC to FORMOSATâ€7/COSMICâ€2. Space Weather, 2014, 12, 616-621.	1.3	81
24	Concentric traveling ionosphere disturbances triggered by Super Typhoon Meranti (2016). Geophysical Research Letters, 2017, 44, 1219-1226.	1.5	80
25	Coseismic ionospheric disturbances triggered by the Chi hi earthquake. Journal of Geophysical Research, 2010, 115, .	3.3	78
26	Tsunamigenic ionospheric hole. Geophysical Research Letters, 2012, 39, .	1.5	78
27	Atmospheric anomalies observed during earthquake occurrences. Geophysical Research Letters, 2004, 31, n/a-n/a.	1.5	76
28	Assimilation of FORMOSATâ€3/COSMIC electron density profiles into a coupled thermosphere/ionosphere model using ensemble Kalman filtering. Journal of Geophysical Research, 2012, 117, .	3.3	74
29	Observations and simulations of seismoionospheric GPS total electron content anomalies before the 12 January 2010 <i>M</i> 7 Haiti earthquake. Journal of Geophysical Research, 2011, 116, n/a-n/a.	3.3	73
30	Solar flare signatures of the ionospheric GPS total electron content. Journal of Geophysical Research, 2006, 111, .	3.3	72
31	Statistics of geomagnetic storms and ionospheric storms at low and mid latitudes in two solar cycles. Journal of Geophysical Research, 2011, 116, n/a-n/a.	3.3	72
32	Large-scale variations of the low-latitude ionosphere during the October-November 2003 superstorm: Observational results. Journal of Geophysical Research, 2005, 110, .	3.3	71
33	Artificial plasma cave in the low″atitude ionosphere results from the radio occultation inversion of the FORMOSATâ€3/COSMIC. Journal of Geophysical Research, 2010, 115, .	3.3	71
34	An empirical model of the quiet daily geomagnetic field variation. Journal of Geophysical Research, 2011, 116, n/a-n/a.	3.3	71
35	lonospheric foF2 and TEC Anomalous Days Associated with M >= 5.0 Earthquakes in Taiwan during 1997-1999. Terrestrial, Atmospheric and Oceanic Sciences, 2004, 15, 371.	0.3	71
36	Physical mechanisms of the ionospheric storms at equatorial and higher latitudes during the recovery phase of geomagnetic storms. Journal of Geophysical Research: Space Physics, 2013, 118, 2660-2669.	0.8	69

#	Article	IF	CITATIONS
37	Ionospheric solar flare effects monitored by the ground-based GPS receivers: Theory and observation. Journal of Geophysical Research, 2004, 109, .	3.3	67
38	Causal link of the waveâ€4 structures in plasma density and vertical plasma drift in the low″atitude ionosphere. Journal of Geophysical Research, 2009, 114, .	3.3	64
39	The vertical propagation of disturbances triggered by seismic waves of the 11 March 2011 <i>M</i> 9.0 Tohoku earthquake over Taiwan. Geophysical Research Letters, 2016, 43, 1759-1765.	1.5	63
40	Reduction of electron temperature in low″atitude ionosphere at 600 km before and after large earthquakes. Journal of Geophysical Research, 2008, 113, .	3.3	60
41	Global S4 index variations observed using FORMOSATâ€3/COSMIC GPS RO technique during a solar minimum year. Journal of Geophysical Research, 2012, 117, .	3.3	60
42	Statistical Tests for Pre-earthquake Ionospheric Anomaly. Terrestrial, Atmospheric and Oceanic Sciences, 2004, 15, 385.	0.3	59
43	Comparisons of GPS/MET retrieved ionospheric electron density and ground based ionosonde data. Earth, Planets and Space, 2001, 53, 193-205.	0.9	58
44	Statistical investigation of the saturation effect in the ionospheric foF2 versus sunspot, solar radio noise, and solar EUV radiation. Journal of Geophysical Research, 2003, 108, .	3.3	58
45	The effects of the pre-reversal ExB drift, the EIA asymmetry, and magnetic activity on the equatorial spread F during solar maximum. Annales Geophysicae, 2005, 23, 745-751.	0.6	57
46	A study of tomographically reconstructed ionospheric images during a solar eclipse. Journal of Geophysical Research, 1999, 104, 79-94.	3.3	56
47	Stationary planetary wave and nonmigrating tidal signatures in ionospheric wave 3 and wave 4 variations in 2007–2011 FORMOSATâ€3/COSMIC observations. Journal of Geophysical Research: Space Physics, 2013, 118, 6651-6665.	0.8	54
48	Observational evidence of ionospheric migrating tide modification during the 2009 stratospheric sudden warming. Geophysical Research Letters, 2012, 39, .	1.5	53
49	Long-distance propagation of ionospheric disturbance generated by the 2011 off the Pacific coast of Tohoku Earthquake. Earth, Planets and Space, 2011, 63, 881-884.	0.9	52
50	Temporal and spatial precursors in the ionospheric global positioning system (GPS) total electron content observed before the 26 December 2004 M9.3 Sumatra–Andaman Earthquake. Journal of Geophysical Research, 2010, 115, .	3.3	51
51	Ionosphere disturbances observed throughout Southeast Asia of the superstorm of 20–22 November 2003. Journal of Geophysical Research, 2008, 113, .	3.3	50
52	New aspects of thermospheric and ionospheric storms revealed by CHAMP. Journal of Geophysical Research, 2011, 116, n/a-n/a.	3.3	49
53	Ionospheric assimilation of radio occultation and ground-based GPS data using non-stationary background model error covariance. Atmospheric Measurement Techniques, 2015, 8, 171-182.	1.2	49
54	The solar flare radiation responsible for sudden frequency deviation and geomagnetic fluctuation. Journal of Geophysical Research, 1996, 101, 10855-10862.	3.3	48

#	Article	IF	CITATIONS
55	The Early Results and Validation of FORMOSATâ€7/COSMICâ€2 Space Weather Products: Global Ionospheric Specification and Neâ€Aided Abel Electron Density Profile. Journal of Geophysical Research: Space Physics, 2020, 125, e2020JA028028.	0.8	47
56	Longitudinal development of lowâ€latitude ionospheric irregularities during the geomagnetic storms of July 2004. Journal of Geophysical Research, 2010, 115, .	3.3	44
57	The climatology of ionospheric plasma bubbles and irregularities over Brazil. Annales Geophysicae, 2005, 23, 379-384.	0.6	43
58	Characterizing the 10 November 2004 stormâ€ŧime middleâ€latitude plasma bubble event in Southeast Asia using multiâ€instrument observations. Journal of Geophysical Research, 2009, 114, .	3.3	43
59	Effects of inferring unobserved thermospheric and ionospheric state variables by using an Ensemble Kalman Filter on global ionospheric specification and forecasting. Journal of Geophysical Research: Space Physics, 2014, 119, 9256-9267.	0.8	43
60	Ionospheric Bow Wave Induced by the Moon Shadow Ship Over the Continent of United States on 21 August 2017. Geophysical Research Letters, 2018, 45, 538-544.	1.5	43
61	Theoretical study of the ionospheric Weddell Sea Anomaly using SAMI2. Journal of Geophysical Research, 2011, 116, n/a-n/a.	3.3	42
62	Surface Deformation and Seismic Rebound: Implications and Applications. Surveys in Geophysics, 2011, 32, 291-313.	2.1	42
63	Seismo-traveling ionospheric disturbances of ionograms observed during the 2011 M w 9.0 Tohoku Earthquake. Earth, Planets and Space, 2011, 63, 897-902.	0.9	42
64	Explanation of the sporadicâ€ <i>E</i> layer formation by comparing FORMOSATâ€3/COSMIC data with meteor and wind shear information. Journal of Geophysical Research D: Atmospheres, 2014, 119, 4568-4579.	1.2	42
65	Seismo-ionospheric anomalies of the GPS-TEC appear before the 12 May 2008 magnitude 8.0 Wenchuan Earthquake. International Journal of Remote Sensing, 2010, 31, 3579-3587.	1.3	41
66	The ionospheric midlatitude trough observed by FORMOSAT-3/COSMIC during solar minimum. Journal of Geophysical Research, 2011, 116, n/a-n/a.	3.3	41
67	Seismo-ionospheric anomalies in total electron content of the GIM and electron density of DEMETER before the 27 February 2010 M8.8 Chile earthquake. Advances in Space Research, 2013, 51, 2309-2315.	1.2	40
68	Groundwater–strain coupling before the 1999 M w 7.6 Taiwan Chi-Chi earthquake. Journal of Hydrology, 2015, 524, 378-384.	2.3	40
69	Ionospheric data assimilation with thermosphereâ€ionosphereâ€electrodynamics general circulation model and GPSâ€TEC during geomagnetic storm conditions. Journal of Geophysical Research: Space Physics, 2016, 121, 5708-5722.	0.8	40
70	Seasonal and local time variation of ionospheric migrating tides in 2007–2011 FORMOSATâ€3/COSMIC and TIEâ€GCM total electron content. Journal of Geophysical Research: Space Physics, 2013, 118, 2545-2564.	0.8	39
71	lonospheric <i>F</i> ₂ region perturbed by the 25 April 2015 Nepal earthquake. Journal of Geophysical Research: Space Physics, 2016, 121, 5778-5784.	0.8	38
72	The propagation of traveling atmospheric disturbances observed during the April 6-7, 2000 ionospheric storm. Geophysical Research Letters, 2002, 29, 12-1-12-4.	1.5	37

#	Article	IF	CITATIONS
73	lonospheric variability unrelated to solar and geomagnetic activity. Advances in Space Research, 2004, 34, 1926-1933.	1.2	37
74	Seismo-ionospheric precursor of the 2008 Mw7.9 Wenchuan earthquake observed by FORMOSAT-3/COSMIC. GPS Solutions, 2010, 14, 83-89.	2.2	37
75	Latitudinal distribution of anomalous ion density as a precursor of a large earthquake. Journal of Geophysical Research, 2011, 116, n/a-n/a.	3.3	37
76	Bow and stern waves triggered by the Moon's shadow boat. Geophysical Research Letters, 2011, 38, n/a-n/a.	1.5	37
77	Electron density profiles in the equatorial ionosphere observed by the FORMOSAT-3/COSMIC and a digisonde at Jicamarca. GPS Solutions, 2010, 14, 75-81.	2.2	36
78	Propagating planetary wave coupling in SABER MLT temperatures and GPS TEC during the 2005/2006 austral summer. Journal of Geophysical Research, 2011, 116, n/a-n/a.	3.3	36
79	Wind dynamo effects on ground magnetic perturbations and vertical drifts. Journal of Geophysical Research, 2008, 113, .	3.3	35
80	Tracking the epicenter and the tsunami origin with GPS ionosphere observation. Earth, Planets and Space, 2011, 63, 859-862.	0.9	35
81	Infrasound in the ionosphere from earthquakes and typhoons. Journal of Atmospheric and Solar-Terrestrial Physics, 2018, 171, 72-82.	0.6	35
82	Precursory phenomena associated with the 1999 Chi-Chi earthquake in Taiwan as identified under the iSTEP program. Physics and Chemistry of the Earth, 2006, 31, 365-377.	1.2	34
83	Daytime longitudinal structures of electron density and temperature in the topside ionosphere observed by the Hinotori and DEMETER satellites. Journal of Geophysical Research, 2011, 116, .	3.3	34
84	Observations of global ionospheric responses to the 2009 stratospheric sudden warming event by FORMOSATâ€3/COSMIC. Journal of Geophysical Research, 2012, 117, .	3.3	33
85	A possible space-based tsunami early warning system using observations of the tsunami ionospheric hole. Scientific Reports, 2016, 6, 37989.	1.6	33
86	Data Assimilation of Groundâ€Based GPS and Radio Occultation Total Electron Content for Global Ionospheric Specification. Journal of Geophysical Research: Space Physics, 2017, 122, 10,876.	0.8	33
87	The low latitude ionospheric effects of the April 2000 magnetic storm near the longitude 120°E. Earth, Planets and Space, 2004, 56, 607-612.	0.9	32
88	Theoretical study of new plasma structures in the lowâ€latitude ionosphere during a major magnetic storm. Journal of Geophysical Research, 2009, 114, .	3.3	32
89	Pre-seismic geomagnetic anomaly and earthquake location. Tectonophysics, 2010, 489, 240-247.	0.9	32
90	Assessment of the Impact of FORMOSATâ€7/COSMICâ€2 GNSS RO Observations on Midlatitude and Low‣atitude Ionosphere Specification: Observing System Simulation Experiments Using Ensemble Square Root Filter. Journal of Geophysical Research: Space Physics, 2018, 123, 2296-2314.	0.8	32

#	Article	IF	CITATIONS
91	Digisonde spreadFand GPS phase fluctuations in the equatorial ionosphere during solar maximum. Journal of Geophysical Research, 2006, 111, .	3.3	30
92	Modeling and observations of the low latitude ionosphereâ€plasmasphere system at long deep solar minimum. Journal of Geophysical Research, 2012, 117, .	3.3	30
93	Temporal and spatial precursors in ionospheric total electron content of the 16 October 1999 <i>M_w</i> 7.1 Hector Mine earthquake. Journal of Geophysical Research: Space Physics, 2013, 118, 6511-6517.	0.8	30
94	Thermospheric tidal effects on the ionospheric midlatitude summer nighttime anomaly using SAMI3 and TIEGCM. Journal of Geophysical Research: Space Physics, 2013, 118, 3836-3845.	0.8	30
95	Anomalous frequency characteristics of groundwater level before major earthquakes in Taiwan. Hydrology and Earth System Sciences, 2013, 17, 1693-1703.	1.9	30
96	Observation and model comparisons of the traveling atmospheric disturbances over the Western Pacific region during the 6–7 April 2000 magnetic storm. Journal of Geophysical Research, 2004, 109, .	3.3	29
97	Surface displacements in Japan before the 11 March 2011 M9.0 Tohoku-Oki earthquake. Journal of Asian Earth Sciences, 2014, 80, 165-171.	1.0	29
98	Structure and origins of the Weddell Sea Anomaly from tidal and planetary wave signatures in FORMOSATâ€3/COSMIC observations and GAIA GCM simulations. Journal of Geophysical Research: Space Physics, 2015, 120, 1325-1340.	0.8	29
99	The heights of sporadic-E layer simultaneously observed by the VHF radar and ionosondes in Chung-Li. Geophysical Research Letters, 2000, 27, 641-644.	1.5	28
100	Neutral wind effect in producing a storm time ionospheric additional layer in the equatorial ionization anomaly region. Journal of Geophysical Research, 2009, 114, .	3.3	28
101	Ionospheric and thermospheric storms at equatorial latitudes observed by CHAMP, ROCSAT, and DMSP. Journal of Geophysical Research, 2012, 117, .	3.3	28
102	Evaluation of seismo-electric anomalies using magnetic data in Taiwan. Natural Hazards and Earth System Sciences, 2013, 13, 597-604.	1.5	28
103	Ionospheric shock waves triggered by rockets. Annales Geophysicae, 2014, 32, 1145-1152.	0.6	28
104	Modifications of the ionosphere prior to large earthquakes: report from the Ionosphere Precursor Study Group. Geoscience Letters, 2016, 3, .	1.3	28
105	Gigantic Circular Shock Acoustic Waves in the Ionosphere Triggered by the Launch of FORMOSATâ€5 Satellite. Space Weather, 2018, 16, 172-184.	1.3	28
106	Fluctuations on vertical profiles of the ionospheric electron density perturbed by the March 11, 2011 M9.0 Tohoku earthquake and tsunami. GPS Solutions, 2019, 23, 1.	2.2	28
107	Individual Wave Propagations in Ionosphere and Troposphere Triggered by the Hunga Tonga-Hunga Ha'apai Underwater Volcano Eruption on 15 January 2022. Remote Sensing, 2022, 14, 2179.	1.8	28
108	Identification of earthquake signals from groundwater level records using the HHT method. Geophysical Journal International, 2010, 180, 1231-1241.	1.0	27

#	Article	IF	CITATIONS
109	Empirical models of Total Electron Content based on functional fitting over Taiwan during geomagnetic quiet condition. Annales Geophysicae, 2009, 27, 3321-3333.	0.6	27
110	A precursory ULF signature for the Chi-Chi earthquake in Taiwan. Natural Hazards and Earth System Sciences, 2001, 1, 33-36.	1.5	26
111	A comparison of the equatorial spread F derived by the International Reference Ionosphere and the S 4 index observed by FORMOSAT-3/COSMIC during the solar minimum period of 2007–2009. Earth, Planets and Space, 2012, 64, 467-471.	0.9	26
112	Magnetic storm free ULF analysis in relation with earthquakes in Taiwan. Natural Hazards and Earth System Sciences, 2012, 12, 1747-1754.	1.5	26
113	Spread F, GPS phase fluctuations, and plasma bubbles near the crest of equatorial ionization anomaly during solar maximum. Journal of Geophysical Research, 2009, 114, .	3.3	25
114	Worst-Case GPS Scintillations on the Ground Estimated from Radio Occultation Observations of FORMOSAT-3/COSMIC During 2007–2014. Surveys in Geophysics, 2016, 37, 791-809.	2.1	25
115	Global ionosphere map constructed by using total electron content from ground-based GNSS receiver and FORMOSAT-3/COSMIC GPS occultation experiment. GPS Solutions, 2017, 21, 1583-1591.	2.2	25
116	Correlation between electron density and temperature in the topside ionosphere. Journal of Geophysical Research, 2011, 116, n/a-n/a.	3.3	24
117	The neutral temperature in the ionospheric dynamo region and the ionospheric F region density during Wenchuan and Pingtung Doublet earthquakes. Natural Hazards and Earth System Sciences, 2011, 11, 1759-1768.	1.5	24
118	Longâ€ŧerm variations of the nighttime electron density enhancement during the ionospheric midlatitude summer. Journal of Geophysical Research, 2012, 117, .	3.3	24
119	The intermediate layers and associated tidal motions observed by a digisonde in the equatorial anomaly region. Annales Geophysicae, 2003, 21, 1039-1045.	0.6	24
120	Modeling impact of FORMOSATâ€7/COSMICâ€2 mission on ionospheric space weather monitoring. Journal of Geophysical Research: Space Physics, 2013, 118, 6518-6523.	0.8	23
121	Impact of Assimilating the FORMOSATâ€3/COSMIC and FORMOSATâ€7/COSMICâ€2 RO Data on the Midlatitude and Low‣atitude Ionospheric Specification. Earth and Space Science, 2018, 5, 875-890.	1.1	23
122	Variations in the equatorial ionization anomaly peaks in the Western Pacific region during the geomagnetic storms of April 6 and July 15, 2000. Earth, Planets and Space, 2007, 59, 401-405.	0.9	22
123	Modeling the pre-earthquake electrostatic effect on the F region ionosphere. Advances in Space Research, 2012, 50, 1524-1533.	1.2	22
124	A statistical study on the characteristics of ionospheric storms in the equatorial ionization anomaly region: GPSâ€TEC observed over Taiwan. Journal of Geophysical Research: Space Physics, 2013, 118, 3856-3865.	0.8	22
125	Subionospheric VLF/LF Probing of Ionospheric Perturbations Associated with Earthquakes: A Possibility of Earthquake Prediction. SICE Journal of Control Measurement and System Integration, 2010, 3, 10-14.	0.4	22
126	Seismo-Ionospheric Precursors of the 26 December 2006 M 7.0 Pingtung Earthquake Doublet. Terrestrial, Atmospheric and Oceanic Sciences, 2008, 19, 751.	0.3	21

#	Article	IF	CITATIONS
127	Ionospheric electron content and NmF2 from nighttime OI 135.6 nm intensity. Journal of Geophysical Research, 2011, 116, n/a-n/a.	3.3	21

Observation of surface displacements from GPS analyses before and after the Jiashian earthquake (M=) Tj ETQq0 0 $\underset{1.0}{0}$ rgBT /Oyerlock 10 $\underset{1.0}{21}$

129	Ionospheric ripples excited by superimposed wave fronts associated with Rayleigh waves in the thermosphere. Journal of Geophysical Research: Space Physics, 2013, 118, 905-911.	0.8	21
130	Fieldâ€aligned neutral wind bias correction scheme for global ionospheric modeling at midlatitudes by assimilating FORMOSATâ€3/COSMIC <i><scp><i>h_mF</i></scp></i> 2 data under geomagnetically quiet conditions. Journal of Geophysical Research: Space Physics, 2015, 120, 3130-3149.	0.8	21
131	An empirical model of L-band scintillation S4 index constructed by using FORMOSAT-3/COSMIC data. Advances in Space Research, 2017, 60, 1015-1028.	1.2	21
132	Extreme Positive Ionosphere Storm Triggered by a Minor Magnetic Storm in Deep Solar Minimum Revealed by FORMOSATâ€7/COSMICâ€2 and GNSS Observations. Journal of Geophysical Research: Space Physics, 2021, 126, e2020JA028261.	0.8	21
133	Revisiting the Modulations of Ionospheric Solar and Lunar Migrating Tides During the 2009 Stratospheric Sudden Warming by Using Global Ionosphere Specification. Space Weather, 2019, 17, 767-777.	1.3	20
134	Ionospheric positive storm phases at the magnetic equator close to sunset. Journal of Geophysical Research, 2010, 115, .	3.3	19
135	Statistical evidences of seismo-ionospheric precursors applying receiver operating characteristic (ROC) curve on the GPS total electron content in China. Journal of Asian Earth Sciences, 2015, 114, 393-402.	1.0	19
136	On a possible seismomagnetic effect in the topside ionosphere. Advances in Space Research, 2015, 56, 1707-1713.	1.2	19
137	On the Relationship Between <i>E</i> Region Scintillation and ENSO Observed by FORMOSATâ€3/COSMIC. Journal of Geophysical Research: Space Physics, 2018, 123, 4053-4065.	0.8	19
138	A New Instrumental Array in Sichuan, China, to Monitor Vibrations and Perturbations of the Lithosphere, Atmosphere, and Ionosphere. Surveys in Geophysics, 0, , 1.	2.1	19
139	Abnormal infrasound signals before 92M≧ 7.0 worldwide earthquakes during 2002–2008. Journal of Asian Earth Sciences, 2011, 41, 434-441.	1.0	18
140	A statistical study of low latitude <i>F</i> region irregularities at Brazilian longitudinal sector response to geomagnetic storms during postâ€sunset hours in solar cycle 23. Journal of Geophysical Research, 2012, 117, .	3.3	18
141	Groundâ€based GPS observation of SEDâ€associated irregularities over CONUS. Journal of Geophysical Research: Space Physics, 2013, 118, 2478-2489.	0.8	18
142	Morphology of midlatitude electron density enhancement using total electron content measurements. Journal of Geophysical Research: Space Physics, 2016, 121, 1503-1517.	0.8	18
143	Low latitude ionospheric effects near longitude 120°E during the great geomagnetic storm of july 2000. Science in China Series A: Mathematics, 2002, 45, 148-155.	0.5	17
144	Predawn ionospheric heating observed by Hinotori satellite. Journal of Geophysical Research, 2010, 115, .	3.3	17

#	Article	IF	CITATIONS
145	Seismo-Traveling Ionospheric Disturbances Triggered by the 12 May 2008 M 8.0 Wenchuan Earthquake. Terrestrial, Atmospheric and Oceanic Sciences, 2012, 23, 9.	0.3	17
146	Precursory enhancement of EIA in the morning sector: Contribution from mid-latitude large earthquakes in the north-east Asian region. Advances in Space Research, 2016, 57, 268-280.	1.2	17
147	Changes of Geomagnetic Total Field and Occurrences of Earthquakes in Taiwan. Terrestrial, Atmospheric and Oceanic Sciences, 2004, 15, 361.	0.3	17
148	GPS phase fluctuations observed along the American sector during low irregularity activity months of 1997–2000. Earth, Planets and Space, 2002, 54, 141-152.	0.9	16
149	The O I 135.6 nm airglow observations of the midlatitude summer nighttime anomaly by TIMED/GUVI. Journal of Geophysical Research, 2011, 116, n/a-n/a.	3.3	16
150	An integrated study of anomalies observed before four major earthquakes: 2004 Sumatra M9.3, 2006 Pingtung M7.0, 2007 Chuetsu Oki M6.8, and 2008 Wenchuan M8.0. Journal of Asian Earth Sciences, 2011, 41, 401-409.	1.0	16
151	Three-dimensional electron density along the WSA and MSNA latitudes probed by FORMOSAT-3/COSMIC. Earth, Planets and Space, 2015, 67, .	0.9	16
152	A Statistical Study of Lightning Activities and MÂ≥Â5.0 Earthquakes in Taiwan During 1993–2004. Surveys in Geophysics, 2015, 36, 851-859.	2.1	16
153	Electron temperature in nighttime sporadic E layer at mid-latitude. Annales Geophysicae, 2008, 26, 533-541.	0.6	15
154	Anomalous Geomagnetic Variations Possibly Linked with the Taiwan Earthquake (<mml:math) 0="" <br="" etqq0="" rgbt="" tj="">on 19 December 2009. International Journal of Geophysics, 2011, 2011, 1-10.</mml:math)>	Overlock 0.4	10 Tf 50 387 15
155	Temporal and spatial analyses on seismo-electric anomalies associated with the 27 February 2010 <i>M</i> = 8.8 Chile earthquake observed by DEMETER satellite. Natural Hazards and Earth System Sciences, 2013, 13, 3281-3289.	1.5	15
156	Topside ionospheric electron temperature and density along the Weddell Sea latitude. Journal of Geophysical Research: Space Physics, 2015, 120, 609-614.	0.8	15
157	Spaceâ€based imaging of nighttime mediumâ€scale traveling ionospheric disturbances using FORMOSATâ€2/ISUAL 630.0 nm airglow observations. Journal of Geophysical Research: Space Physics, 2016, 121, 4769-4781.	0.8	15
158	A Study of Daytime Lâ€Band Scintillation in Association With Sporadic <i>E</i> Along the Magnetic Dip Equator. Radio Science, 2017, 52, 1570-1577.	0.8	15
159	The Midlatitude Trough and the Plasmapause in the Nighttime Ionosphere Simultaneously Observed by DEMETER During 2006–2009. Journal of Geophysical Research: Space Physics, 2018, 123, 5917-5932.	0.8	15
160	Lunar Tide Effects on Ionospheric Solar Eclipse Signatures: The August 21, 2017 Event as an Example. Journal of Geophysical Research: Space Physics, 2020, 125, e2020JA028472.	0.8	15
161	Determination of Epicenters before Earthquakes Utilizing Far Seismic and GNSS Data: Insights from Ground Vibrations. Remote Sensing, 2020, 12, 3252.	1.8	14
162	Advanced Ionospheric Probe scientific mission onboard FORMOSAT-5 satellite. Terrestrial, Atmospheric and Oceanic Sciences, 2017, 28, 99-110.	0.3	14

#	Article	IF	CITATIONS
163	Resident Waves in the Ionosphere Before the M6.1 Dali and M7.3 Qinghai Earthquakes of 21–22 May 2021. Earth and Space Science, 2022, 9, e2021EA002159.	1.1	14
164	Stratosphere Perturbed by the 2011 Mw9.0 Tohoku Earthquake. Geophysical Research Letters, 2018, 45, 10,050.	1.5	13
165	Tropospheric and Ionospheric Anomalies Induced by Volcanic and Saharan Dust Events as Part of Geosphere Interaction Phenomena. Geosciences (Switzerland), 2019, 9, 177.	1.0	13
166	IDEASSat: A 3U CubeSat mission for ionospheric science. Advances in Space Research, 2020, 66, 116-134.	1.2	13
167	The source detection of 28 September 2018 Sulawesi tsunami by using ionospheric GNSS total electron content disturbance. Geoscience Letters, 2020, 7, .	1.3	13
168	ULF Geomagnetic and Geopotential Measurement at Chia-Yi, Taiwan. Journal of Atmospheric Electricity, 2002, 22, 217-222.	0.1	13
169	Ionospheric Disturbances Triggered by the Mw7.6 Earthquake off the Coast of El Salvador on 13 January 2001. Terrestrial, Atmospheric and Oceanic Sciences, 2006, 17, 345.	0.3	13
170	An observing system simulation experiment for FORMOSAT-5/AIP detecting seismo-ionospheric precursors. Terrestrial, Atmospheric and Oceanic Sciences, 2017, 28, 117-127.	0.3	13
171	Ionospheric disturbance associated with radiation accidents of Fukushima I nuclear power plant damaged by the M9.0 2011 Tohoku Earthquake. Advances in Space Research, 2011, 48, 1613-1616.	1.2	12
172	A comparison of a model using the FORMOSAT-3/COSMIC data with the IRI model. Earth, Planets and Space, 2012, 64, 545-551.	0.9	12
173	Continuous Doppler sounding of the ionosphere during solar flares. Earth, Planets and Space, 2018, 70, .	0.9	12
174	Locating Seismo-Conductivity Anomaly before the 2017 MW 6.5 Jiuzhaigou Earthquake in China Using Far Magnetic Stations. Remote Sensing, 2020, 12, 1777.	1.8	12
175	Unique Pre-Earthquake Deformation Patterns in the Spatial Domains from GPS in Taiwan. Remote Sensing, 2020, 12, 366.	1.8	12
176	Advances in Ionospheric Space Weather by Using FORMOSAT-7/COSMIC-2 GNSS Radio Occultations. Atmosphere, 2022, 13, 858.	1.0	12
177	Global Ionospheric Structure Imaged by FORMOSAT-3/COSMIC: Early Results. Terrestrial, Atmospheric and Oceanic Sciences, 2009, 20, 171.	0.3	11
178	Airglow observations over the equatorial ionization anomaly zone in Taiwan. Annales Geophysicae, 2011, 29, 749-757.	0.6	11
179	First results of the limb imaging of 630.0 nm airglow using FORMOSATâ€2/Imager of Sprites and Upper Atmospheric Lightnings. Journal of Geophysical Research, 2009, 114, .	3.3	10
180	Using the IRI, the MAGIC model, and the co-located ground-based GPS receivers to study ionospheric solar eclipse and storm signatures on July 22, 2009. Earth, Planets and Space, 2012, 64, 513-520.	0.9	10

#	Article	IF	CITATIONS
181	A statistical study on ELFâ€whistlers/emissions and <i>M</i> ≥ 5.0 earthquakes in Taiwan. Journal of Geophysical Research: Space Physics, 2013, 118, 3760-3768.	0.8	10
182	Intensity of low-latitude nighttime F-region ionospheric density irregularities observed by ROCSAT and ground-based GPS receivers in solar maximum. Journal of Atmospheric and Solar-Terrestrial Physics, 2015, 123, 92-101.	0.6	10
183	Medium-scale traveling ionospheric disturbances over Taiwan observed with HF Doppler sounding. Earth, Planets and Space, 2017, 69, .	0.9	10
184	Ionospheric density and velocity anomalies before M ≥ 6.5 earthquakes observed by DEMETER satellite. Journal of Asian Earth Sciences, 2018, 166, 210-222.	1.0	10
185	Ionospheric Response to the 21 May 2012 Annular Solar Eclipse Over Taiwan. Journal of Geophysical Research: Space Physics, 2019, 124, 3623-3636.	0.8	10
186	Critical Issues in Ionospheric Data Quality and Implications for Scientific Studies. Radio Science, 2019, 54, 440-454.	0.8	10
187	Ionospheric GNSS Total Electron Content for Tsunami Warning. Journal of Earthquake and Tsunami, 2019, 13, .	0.7	10
188	The Phase Relationship between ULF Geomagnetic Pulsations and HF Doppler Frequency Shift Oscillations on March 24, 1991 Journal of Geomagnetism and Geoelectricity, 1993, 45, 109-114.	0.8	10
189	E region observations over Chung-Li during the SEEK Campaign. Geophysical Research Letters, 1998, 25, 1805-1808.	1.5	9
190	FORMOSAT-3/COSMIC observations of the ionospheric auroral oval development. GPS Solutions, 2010, 14, 91-97.	2.2	9
191	Seismo-Tsunamigenic Ionospheric Hole Triggered by M 9.0 2011 off the Pacific Coast of Tohoku Earthquake. Terrestrial, Atmospheric and Oceanic Sciences, 2012, 23, 327.	0.3	9
192	Potential relationships between seismo-deformation and seismo-conductivity anomalies. Journal of Asian Earth Sciences, 2015, 114, 327-337.	1.0	9
193	Precursor effect of March 11, 2011 off the coast of Tohoku earthquake on high and low latitude ionospheres and its possible disturbing mechanism. Advances in Space Research, 2019, 63, 2623-2637.	1.2	9
194	Wave Steepening in Ionospheric Total Electron Density due to the 21 August 2017 Total Solar Eclipse. Journal of Geophysical Research: Space Physics, 2021, 126, e2020JA028931.	0.8	9
195	Detecting the Ionospheric Disturbances in Japan Using the Threeâ€Dimensional Computerized Tomography. Journal of Geophysical Research: Space Physics, 2021, 126, e2020JA028561.	0.8	9
196	Integrated Search for Taiwan Earthquake Precursors (iSTEP). IEEJ Transactions on Fundamentals and Materials, 2016, 136, 214-220.	0.2	9
197	Oscillations in Ionospheric Virtual Height, Echo Amplitude and Doppler Velocity: Theory and Observations Journal of Geomagnetism and Geoelectricity, 1993, 45, 207-217.	0.8	8
198	Effects of anisotropy and power spectrum of refractivity irregularities on the determination of layer thickness and layer position using the frequency domain interferometry technique. Radio Science, 1997, 32, 437-451.	0.8	8

#	Article	IF	CITATIONS
199	VHF radar and MF/HF dynasonde observations during Polar Mesosphere Summer Echoes conditions at EISCAT. Earth, Planets and Space, 2002, 54, 691-698.	0.9	8
200	Appearance and extension of airglow depletions. Journal of Geophysical Research, 2010, 115, .	3.3	8
201	Ionospheric plasma caves under the equatorial ionization anomaly. Journal of Geophysical Research, 2012, 117, .	3.3	8
202	Does an ionospheric hole appear after an inland earthquake?. Journal of Geophysical Research: Space Physics, 2015, 120, 9998-10005.	0.8	8
203	Multiple seismo-anomalies associated with the M6.1 Ludian earthquake on August 3, 2014. Journal of Asian Earth Sciences, 2015, 114, 352-361.	1.0	8
204	Response of Ionospheric Equatorial Ionization Crests to Lunar Phase. Geophysical Research Letters, 2020, 47, e2019GL086862.	1.5	8
205	Observations of plasma depletions in 557.7â€nm images over Kavalur. Journal of Geophysical Research, 2007, 112, .	3.3	7
206	Possible interaction between thermal electrons and vibrationally excited N ₂ in the lower E-region. Annales Geophysicae, 2011, 29, 583-590.	0.6	7
207	Instantaneous phase shift of annual subsurface temperature cycles derived by the Hilbertâ€Huang transform. Journal of Geophysical Research D: Atmospheres, 2015, 120, 1670-1677.	1.2	7
208	Superposition Property of the Ionospheric Scintillation S4 Index. IEEE Geoscience and Remote Sensing Letters, 2020, 17, 597-600.	1.4	7
209	New algorithms to estimate electron temperature and electron density with contaminated DC Langmuir probe onboard CubeSat. Advances in Space Research, 2020, 66, 148-161.	1.2	7
210	Magnetic Pulsations Triggered by Microseismic Ground Motion. Journal of Geophysical Research: Solid Earth, 2021, 126, e2020JB021416.	1.4	7
211	Spatiotemporal changes of seismicity rate during earthquakes. Natural Hazards and Earth System Sciences, 2020, 20, 3333-3341.	1.5	7
212	Plasma Depletion Bays in the Equatorial Ionosphere Observed by FORMOSATâ€3/COSMIC During 2007–2014. Journal of Geophysical Research: Space Physics, 2020, 125, e2019JA027501.	0.8	6
213	Theoretical study of the ionospheric plasma cave in the equatorial ionization anomaly region. Journal of Geophysical Research: Space Physics, 2014, 119, 10,324.	0.8	5
214	Abnormal Signatures Recorded by FORMOSAT-2 and FORMOSAT-3 over South Atlantic Anomaly and Polar Region. Terrestrial, Atmospheric and Oceanic Sciences, 2014, 25, 573.	0.3	5
215	Low″atitude midnight brightness in 630.0 nm limb observations by FORMOSATâ€2/ISUAL. Journal of Geophysical Research: Space Physics, 2014, 119, 4894-4904.	0.8	5
216	Electron density profiles probed by radio occultation of FORMOSAT-7/COSMIC-2 at 520 and 800 km altitude. Atmospheric Measurement Techniques, 2015, 8, 3069-3074.	1.2	5

#	Article	IF	CITATIONS
217	The fast development of solar terrestrial sciences in Taiwan. Geoscience Letters, 2016, 3, .	1.3	5
218	Artificial magnetic disturbance from the mass rapid transit system in Taiwan. Terra Nova, 2017, 29, 306-311.	0.9	5
219	Implication of Tidal Forcing Effects on the Zonal Variation of Solstice Equatorial Plasma Bubbles. Journal of Geophysical Research: Space Physics, 2021, 126, e2020JA028295.	0.8	5
220	Novel approaches of magnetic inversion using seismic tomography in Taiwan area. Physics of the Earth and Planetary Interiors, 2021, 312, 106663.	0.7	5
221	Ionospheric Observations of the Solar Eclipse on Oct. 24, 1995 at Chung-Li. Terrestrial, Atmospheric and Oceanic Sciences, 1997, 8, 221.	0.3	5
222	Co-seismic signatures in magnetometer, geophone, and infrasound data during the Meinong Earthquake. Terrestrial, Atmospheric and Oceanic Sciences, 2017, 28, 683-692.	0.3	5
223	A Note on the Phase Relationship between ULF Geomagnetic Pulsations and HF-Doppler Oscillations Owing to the Compressional Mechanism Journal of Geomagnetism and Geoelectricity, 1991, 43, 777-781.	0.8	5
224	Co-seismic geomagnetic fluctuations and atmospheric disturbances during the 2018 M 6.2 Hualien Earthquake. Terrestrial, Atmospheric and Oceanic Sciences, 2019, 30, 449-465.	0.3	5
225	OH Airglow and Equatorial Variations Observed by ISUAL Instrument on Board the FORMOSAT 2 Satellite. Terrestrial, Atmospheric and Oceanic Sciences, 2010, 21, 985.	0.3	4
226	Reply to comment by F. Masci and J. N. Thomas on "Temporal and spatial precursors in ionospheric total electron content of the 16 October 1999 <i>M_w</i> 7.1 Hector Mine earthquake― Journal of Geophysical Research: Space Physics, 2014, 119, 6998-7004.	0.8	4
227	Sentinel-1 interferometry with ionospheric correction from global and local TEC maps for land displacement detection in Taiwan. Advances in Space Research, 2020, 65, 1447-1465.	1.2	4
228	Equatorial ionization anomaly response to lunar phase and stratospheric sudden warming. Scientific Reports, 2021, 11, 14695.	1.6	4
229	Comparisons Between Air and Subsurface Temperatures in Taiwan for the Past Century: A Global Warming Perspective. , 2011, , 185-199.		4
230	An observing system simulation experiment for FORMOSAT-5/AIP probing topside ionospheric plasma irregularities by using DEMETER/IAP. Terrestrial, Atmospheric and Oceanic Sciences, 2017, 28, 111-116.	0.3	4
231	Statistical analysis of earthquakes after the 1999 MW 7.7 Chi-Chi, Taiwan, earthquake based on a modified Reasenberg–Jones model. Journal of Asian Earth Sciences, 2015, 114, 299-304.	1.0	3
232	Global Distribution of Persistence of Total Electron Content Anomaly. Atmosphere, 2019, 10, 297.	1.0	3
233	Large air pressure changes triggered by P-SV ground motion in a cave in northern Taiwan. Scientific Reports, 2021, 11, 12850.	1.6	3
234	Onset Altitudes of Coâ€Seismic Ionospheric Disturbances Determined by Multiple Distributions of GNSS TEC After the Foreshock of the 2011 Tohoku Earthquake on March 9, 2011. Earth and Space Science, 2021, 8, e2020EA001217.	1.1	3

#	Article	IF	CITATIONS
235	The impact of FORMOSAT-5/AIP observations on the ionospheric space weather. Terrestrial, Atmospheric and Oceanic Sciences, 2017, 28, 129-137.	0.3	3
236	Lessons Learned from IDEASSat: Design, Testing, on Orbit Operations, and Anomaly Analysis of a First University CubeSat Intended for Ionospheric Science. Aerospace, 2022, 9, 110.	1.1	3
237	Numerical solution for cosmological evolution of Newton's gravitational constant in superstring theories. Physical Review D, 1990, 41, 1329-1332.	1.6	2
238	A study of quasi-16-day ionospheric oscillations. Radiophysics and Quantum Electronics, 1996, 39, 155-165.	0.1	2
239	Vertical group and phase velocities of ionospheric waves derived from the MU radar. Radio Science, 2007, 42, .	0.8	2
240	Development and verification of an innovative photomultiplier calibration system with a 10-fold increase in photometer resolution. Advances in Space Research, 2018, 61, 2673-2679.	1.2	2
241	An algorithm for deriving the electron temperature and electron density probed by Langmuir probe onboard cube satellites. Advances in Space Research, 2020, 66, 135-147.	1.2	2
242	Ionospheric Responses to the July 15 - 16, 2000 Magnetic Storm around Geographic Longitude 121ËšE. Terrestrial, Atmospheric and Oceanic Sciences, 2008, 19, 425.	0.3	2
243	Ionospheric tilting of 21 August 2017 total solar eclipse sounded by GNSS ground-based receivers and radio occultation. Terrestrial, Atmospheric and Oceanic Sciences, 2021, 32, 531.	0.3	2
244	A global model for the occurrence probability of L-band scintillation S4-index. Terrestrial, Atmospheric and Oceanic Sciences, 2021, 32, .	0.3	2
245	Global Ultra-Low-Frequency Geomagnetic Pulsations Associated with the March 24, 1991 Geomagnetic Storm. Terrestrial, Atmospheric and Oceanic Sciences, 2008, 19, 291.	0.3	1
246	A Statistical Comparison of Zonal Mean and Tidal Signatures in FORMOSAT-3/COSMIC and Ground-Based GPS TECs. Terrestrial, Atmospheric and Oceanic Sciences, 2013, 24, 253.	0.3	1
247	Understanding Magnetic Cloud Structure From Shock/Discontinuity Analysis. Journal of Geophysical Research: Space Physics, 2018, 123, 6130-6147.	0.8	1
248	Assessment of Space–Time Hazard of Large Aftershocks of the 2008 Mw7.9 Wenchuan Earthquake. Pure and Applied Geophysics, 2020, 177, 27-36.	0.8	1
249	Evaluation of aftershock hazard of the 2018 M 6.2 Hualien earthquake. Terrestrial, Atmospheric and Oceanic Sciences, 2019, 30, 411-421.	0.3	1
250	Intensive GNSS radio occultation observations by FORMOSAT-7/COSMIC-2 in the dawn, noon, dusk, and midnight ionosphere. Terrestrial, Atmospheric and Oceanic Sciences, 2021, 32, .	0.3	1
251	Severe weather disasters in China linked to solar activity during 1-1825 Common Era. Geoscience Letters, 2022, 9, .	1.3	1
252	Instantaneous amplitude of low-latitude ionospheric irregularities probed by ROCSAT-1, DEMETER, and FORMOSAT-7/COSMIC-2. Advances in Space Research, 2022, 70, 723-732.	1.2	1

#	Article	IF	CITATIONS
253	An error analysis on nature and radar system noises in deriving the phase and group velocities of vertical propagation waves. Earth, Planets and Space, 2013, 65, 911-916.	0.9	Ο
254	Innovative airglow instrument based on constant photon count control. Advances in Space Research, 2021, 68, 105-116.	1.2	0
255	An Automatic Infrared Sensor System to Observe Unusual Animal Behavior. Journal of Atmospheric Electricity, 2002, 22, 223-232.	0.1	Ο